

## Supporting Information

# Durable silver nanowire transparent electrodes enabled by biorenewable nanocoating using chitin and cellulose nanofibers for flexible electronics

*Yoo-Bin Kwon,<sup>a</sup> Seongwon Cho,<sup>b</sup> Dal-Hee Min,<sup>a\*</sup> and Young-Kwan Kim<sup>b\*</sup>*

<sup>a</sup>Department of Chemistry, Seoul National University, Seoul 08826, Republic of Korea

<sup>b</sup>Department of Chemistry, Dongguk University, 30 Pildong-ro, Jung-gu, Seoul, 04620, Republic of Korea

\* To whom correspondence should be addressed.

Prof. Dal-Hee Min, E-mail: dalheemin@snu.ac.kr

Prof. Young-Kwan Kim, E-mail: kimyk@dongguk.edu

## Supporting figures

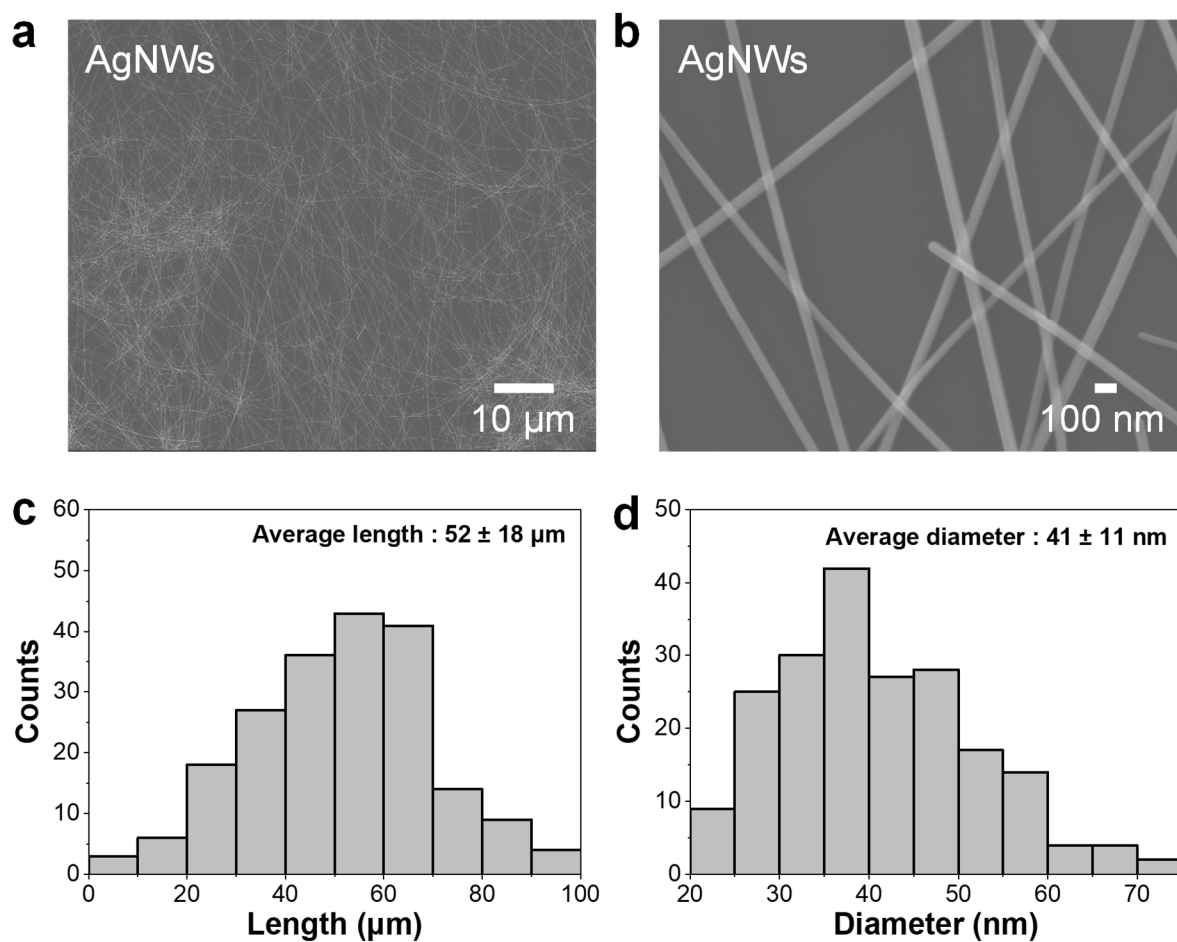


**Fig. S1** (a), (b) SEM images, (c) length and (d) diameter histograms of AgNWs. The as-prepared AgNW has the average length and diameter of  $52 \pm 18 \mu\text{m}$  and  $41 \pm 11 \text{ nm}$ , respectively.

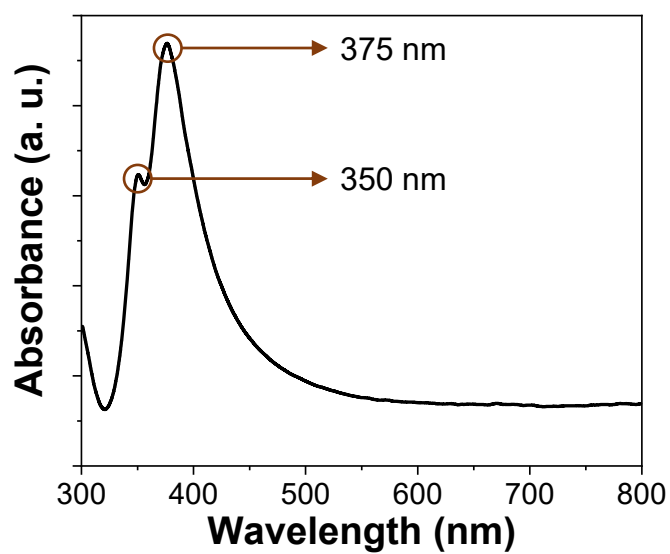


**Fig. S2** UV-Vis spectrum of AgNWs suspension. The UV-Vis spectrum of AgNWs showed two representative absorption bands at 350 and 375 nm, originating from their longitudinal plasmon resonance mode, similar to that of bulk silver, and transverse plasmon resonance mode, respectively.

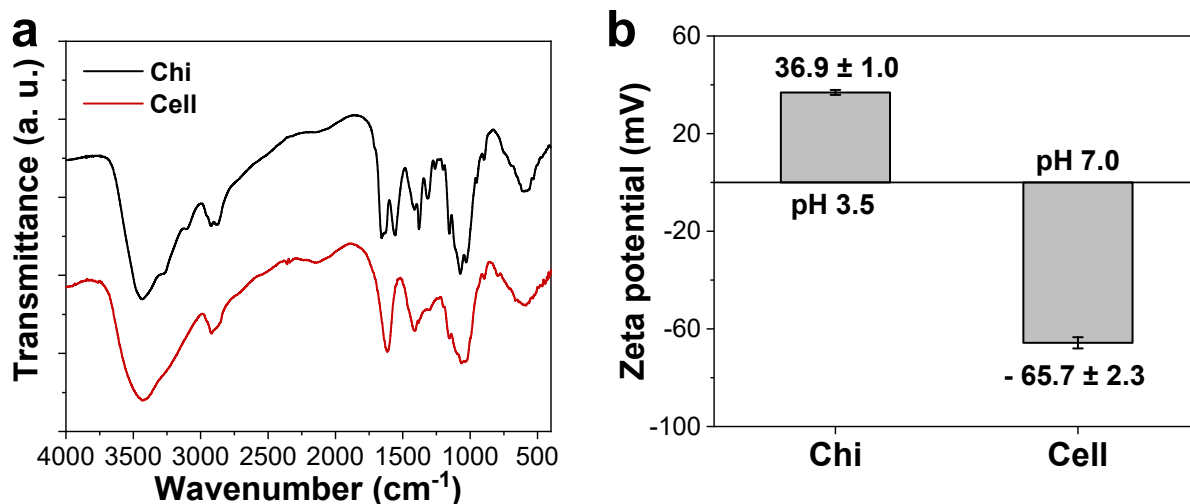


**Fig. S3** (a) FT-IR spectra and (b) zeta potential values of Chi and Cell. In their FT-IR spectra, Chi exhibited the characteristic peaks of  $\alpha$ -chitin at 3432 cm<sup>-1</sup> from O-H stretching, 3266 and 3104 cm<sup>-1</sup> from N-H stretching, 2921 and 2871 cm<sup>-1</sup> from asymmetric (-CH<sub>2</sub>-) and symmetric stretching (-CH<sub>3</sub>), 1656 and 1627 cm<sup>-1</sup> from C=O stretching (amide I), 1556 cm<sup>-1</sup> from N-H bending (amide II), and 1311 cm<sup>-1</sup> from C-N stretching (amide III).<sup>1</sup> Cell exhibited the typical peaks of TEMPO-mediated oxidized cellulose at 3423 cm<sup>-1</sup> from O-H stretching, 2917 and 2852 cm<sup>-1</sup> from asymmetric (-CH<sub>2</sub>-) and symmetric stretching (-CH<sub>3</sub>), 1617 cm<sup>-1</sup> from C=O stretching, 1411 and 1382 cm<sup>-1</sup> from C-H bending, and 1066 cm<sup>-1</sup> from C-O-C stretching.<sup>2,3</sup> Zeta potential values of Chi and Cell were 36.9 ± 1.0 at pH 3.5 and -65.7 ± 2.3 mV at pH 7.0, respectively. These opposite charges facilitate their LBL assembly.

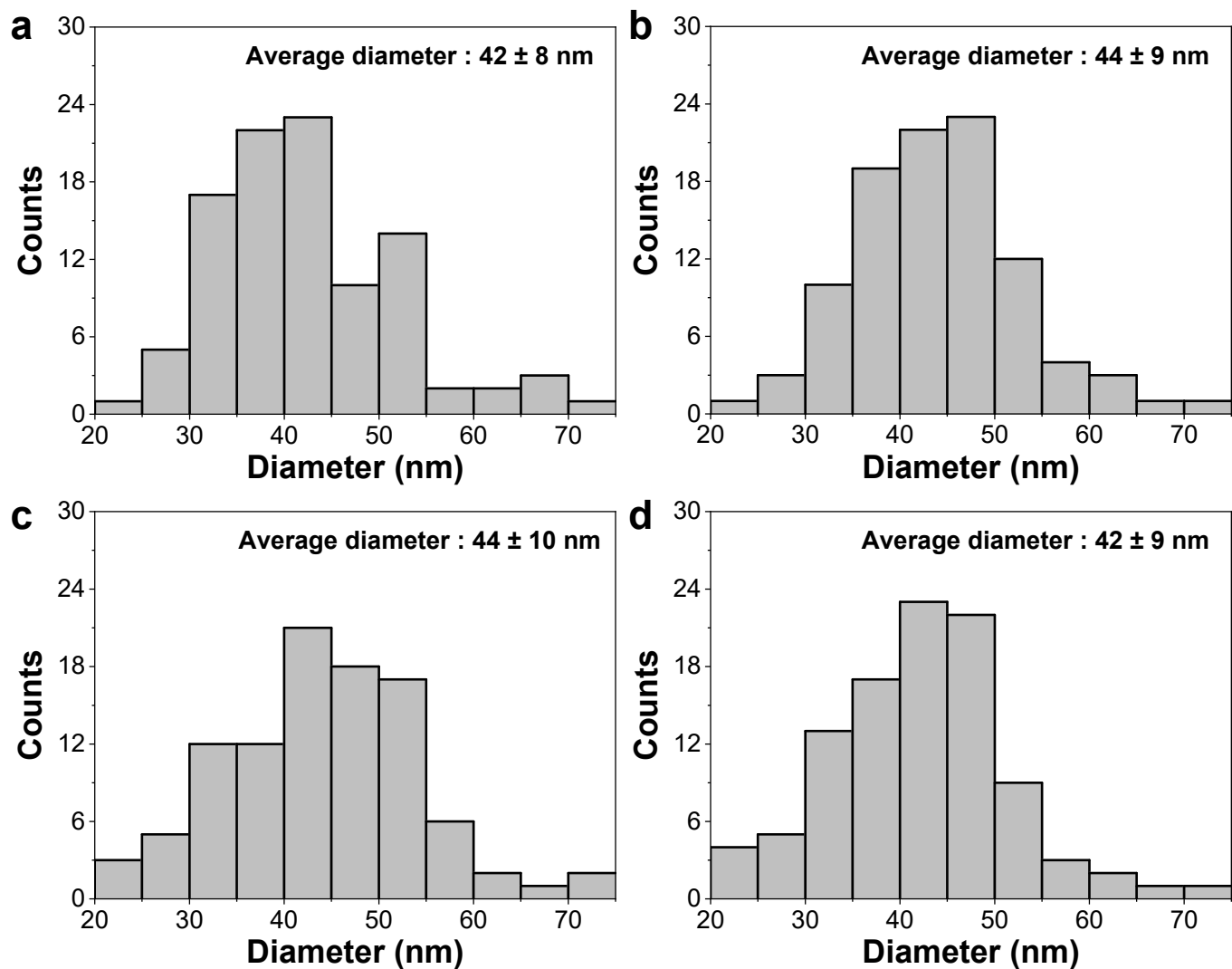


**Fig. S4** Diameter histograms of AgNWs in (a)  $(\text{Chi}/\text{Cell})_1@Al\text{-AgNW}$ , (b)  $(\text{Chi}/\text{Cell})_5@Al\text{-AgNW}$ , (c)  $(\text{Chi}/\text{Cell})_{10}@Al\text{-AgNW}$ , and (d)  $(\text{Chi}/\text{Cell})_{15}@Al\text{-AgNW}$  TEs.

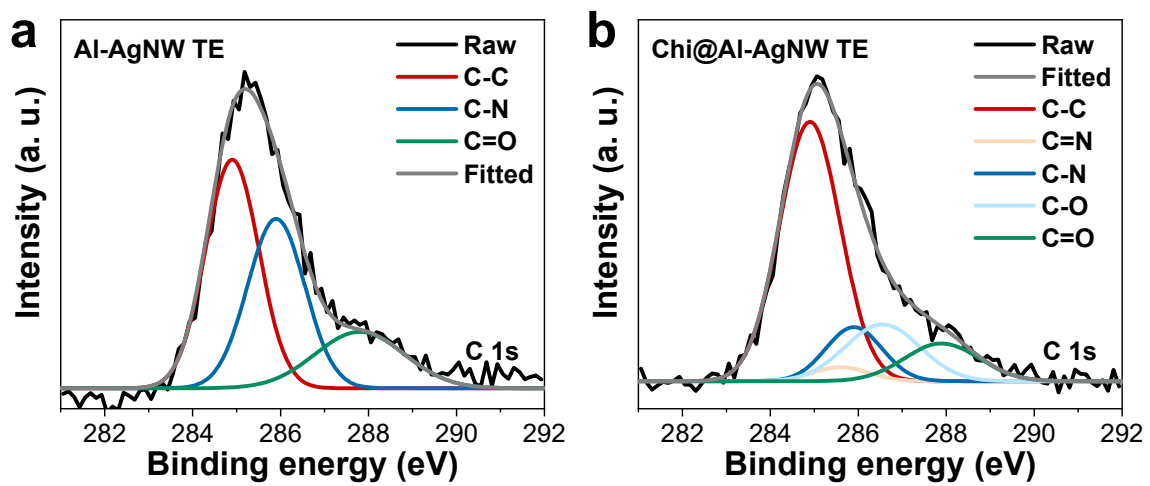


**Fig. S5** C 1s XPS spectra of (a) Al-AgNW and (b) Chi@Al-AgNW TEs.

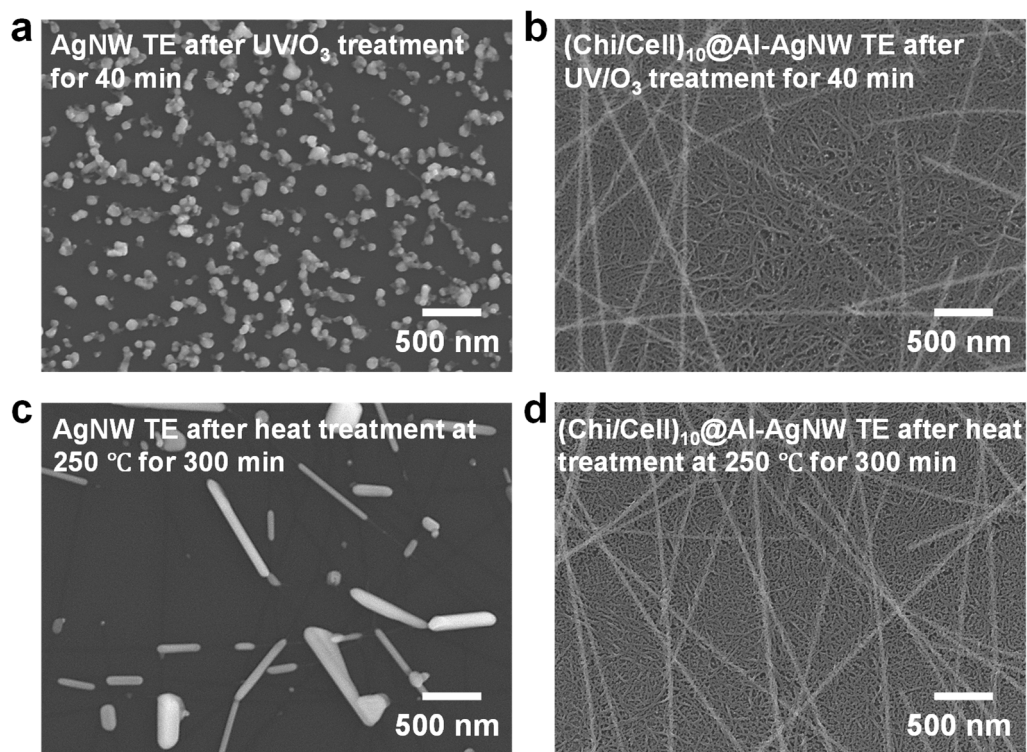


**Fig. S6** SEM images of (a) AgNW and (b) (Chi/Cell)<sub>10</sub>@Al-AgNW TEs after UV/O<sub>3</sub> treatment at 250 °C for 40 min. SEM images of (c) AgNW and (d) (Chi/Cell)<sub>10</sub>@Al-AgNW TEs after heat treatment for 300 min.

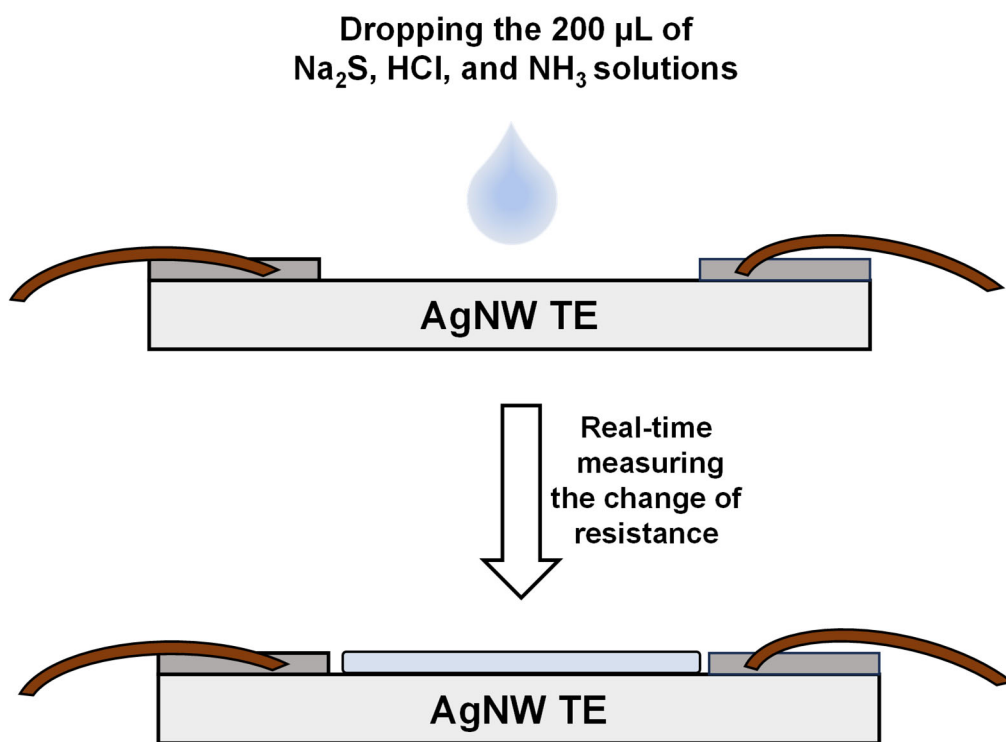


**Fig. S7** Schematic diagram of the method for chemical stability tests.



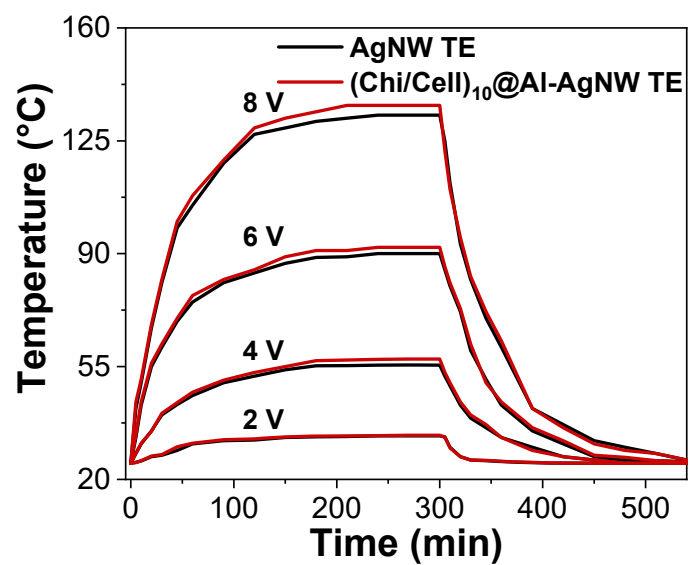


**Fig. S8** Temperature profiles on AgNW and (Chi/Cell)<sub>10</sub>@Al-AgNW TEs as a function of time with different applied voltages at 2, 4, 6, and 8 V.

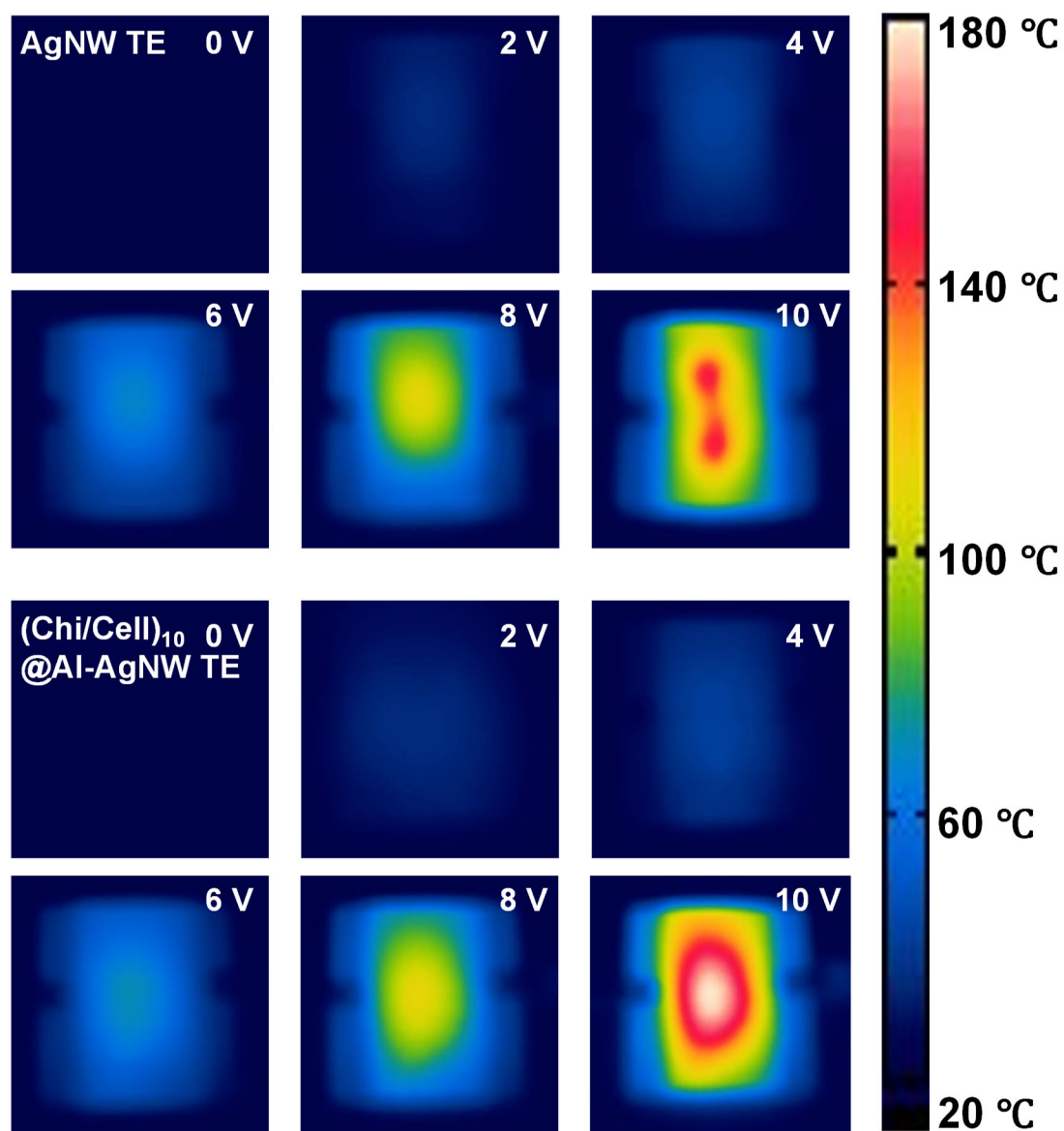


**Fig. S9** Infrared images of AgNW and (Chi/Cell)<sub>10</sub>@Al-AgNW TEs corresponding to the different applied DC voltages.

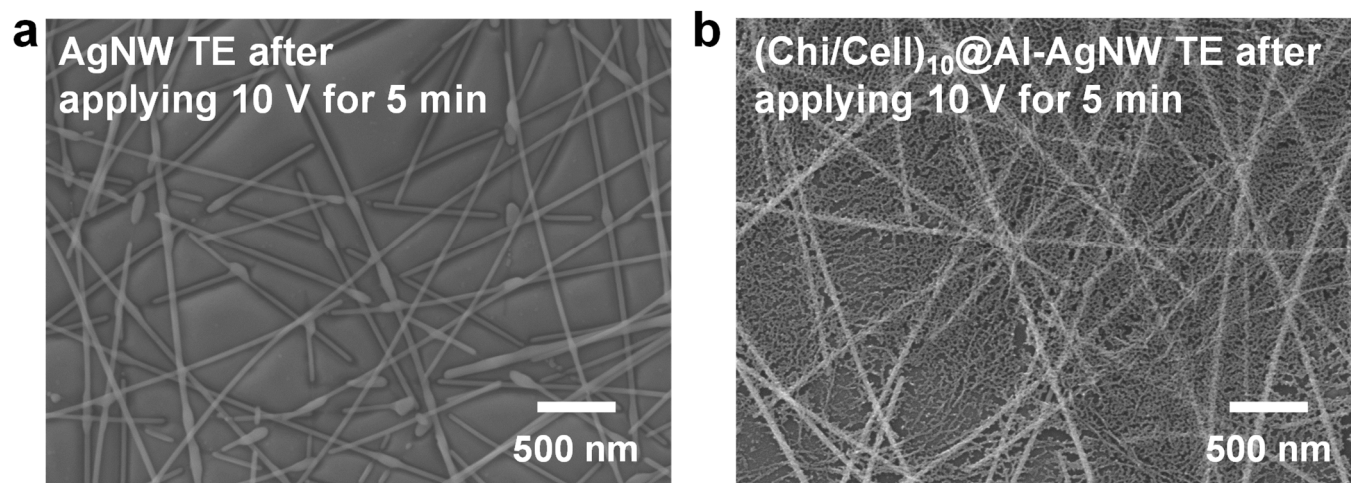


**Fig. S10** SEM images of (a) AgNW and (b) (Chi/Cell)<sub>10</sub>@Al-AgNW TEs after applying 10 V for 5 min.

Sample	C-C (%)	C=N (%)	C-N (%)	C-O (%)	C=O(%)
AgNW TE	51.8	0	40.2	0	8.0
Al-AgNW TE	45.3	0	36.0	0	18.7
Chi@Al-AgNW TE	59.2	2.9	11.4	16.0	10.5
(Chi/Cell) <sub>1</sub> @Al-AgNW TE	56.1	2.1	8.4	23.0	10.4
(Chi/Cell) <sub>5</sub> @Al-AgNW TE	35.4	0.2	23.6	24.4	16.4
(Chi/Cell) <sub>10</sub> @Al-AgNW TE	33.4	0	24.2	25.5	16.9
(Chi/Cell) <sub>15</sub> @Al-AgNW TE	31.1	0	25.5	26.4	17.0

**Table S1.** Relative composition of C–C, C=N, C–N, C–O, and C=O bonds in AgNW, Al-AgNW, Chi, (Chi/Cell)<sub>1</sub>, (Chi/Cell)<sub>5</sub>, (Chi/Cell)<sub>10</sub>, and (Chi/Cell)<sub>15</sub> @Al-AgNW TEs.

Sample	Ag 3d (At%)	C 1s (At%)	N 1s (At%)	O 1s (At%)
AgNW TE	6.5	37.3	5.0	51.2
Al-AgNW TE	6.5	39.1	5.3	49.1
Chi@Al-AgNW TE	6.1	45.7	5.0	43.2
(Chi/Cell) <sub>1</sub> @Al-AgNW TE	5.3	46.0	6.4	42.3
(Chi/Cell) <sub>5</sub> @Al-AgNW TE	1.6	57.0	4.3	37.1
(Chi/Cell) <sub>10</sub> @Al-AgNW TE	0	59.3	4.9	35.8
(Chi/Cell) <sub>15</sub> @Al-AgNW TE	0	60.0	4.9	35.1

**Table S2.** Elemental composition analysis results of AgNW, Al-AgNW, Chi, (Chi/Cell)<sub>1</sub>, (Chi/Cell)<sub>5</sub>, (Chi/Cell)<sub>10</sub>, and (Chi/Cell)<sub>15</sub> @Al-AgNW TEs.

Sample	FoM	Reference
<b>This work (AgNW)</b>	232	
<b>This work ((Chi/Cell)<sub>n</sub>@Al-AgNW)</b>	240 (n=1) 246 (n=5) 246 (n=10) 254 (n=15)	
<b>AION/AgNW</b>	464	4
<b>AgNW/propolis</b>	340	5
<b>AgNW/Chi–LaA</b>	319	6
<b>ul-AgNWs</b>	339	7
<b>LPMN AgNWs</b>	286	8
<b>MoO<sub>x</sub>/AgNW/MoO<sub>x</sub></b>	256	9
<b>(CNF/AL)<sub>10</sub>@Al-AgNW</b>	204	1
<b>Aa-PDA/AgNW</b>	200	10
<b>PEDOT:PSS/AgNW</b>	154	11
<b>EPD-GO/AgNW/GO</b>	150	12
<b>PEDOT:PSS/AgNW</b>	150	13
<b>AgNW</b>	134	14
<b>PPh<sub>3</sub>/AgNW</b>	110	15
<b>Ti/AgNW</b>	89	16
<b>GO/AgNW</b>	71	17
<b>MUA/AgNW</b>	59	18
<b>Graphene</b>	49	19
<b>Commercial ITO</b>	~ 100	20
<b>Minimum requirement value for industry</b>	≥ 35	21

**Table S3.** The FoM values of AgNW, (Chi/Cell)<sub>n</sub>@Al-AgNW TEs, and TEs in other literatures.

## References

- (1) Y. B. Kwon, J. H. Kim and Y. K. Kim, *ACS Appl. Mater. Interfaces*, 2022, **14**, 25993–26003.
- (2) Z. Ur Rehman, A. K. Niaz, J. Il Song and B. Heun Koo, *Polymers*, 2021, **13**, 303.
- (3) T. Thi Thanh Hop, D. Thi Mai, T. Duc Cong, T. Thi Y. Nhi, V. Duc Loi, N. Thi Mai Huong and N. Trinh Tung, *Results Chem.*, 2022, **4**, 100540.
- (4) J. J. Patil, M. L. Reese, E. Lee and J. C. Grossman, *ACS Appl. Mater. Interfaces*, 2022, **14**, 4423–4433.
- (5) Y. Qin, L. Yao, F. Zhang, R. Li, Y. Chen, Y. Chen, T. Cheng, W. Lai, B. Mi, X. Zhang and W. Huang, *ACS Appl. Mater. Interfaces*, 2022, **14**, 38021–38030.
- (6) K. Wang, Y. Jin, B. Qian, J. Wang and F. Xiao, *J. Mater. Chem. C*, 2020, **8**, 4372–4384.
- (7) M. Yao, L. Zhao, C. Fan, X. Han, Z. Wu, H. Sun, G. Wang and R. Xiao, *Chem. Commun.*, 2024, **60**, 8884–8887.
- (8) M. Du, Z. Yang, Y. Miao, C. Wang, P. Dong, H. Wang and K. Guo, *Adv. Funct. Mater.*, 2024, 2404567. <https://doi.org/10.1002/adfm.202404567>
- (9) S. Yu, X. Liu, M. Wu, H. Dong, X. Wang and L. Li, *ACS Appl. Mater. Interfaces*, 2021, **13**, 14470–14478.
- (10) Y. Jin, D. Deng, Y. Cheng, L. Kong and F. Xiao, *Nanoscale*, 2014, **6**, 4812–4818.
- (11) J. E. Lim, S. M. Lee, S. S. Kim, T. W. Kim, H. W. Koo and H. K. Kim, *Sci. Rep.*, 2017, **7**, 14685.
- (12) W. H. Chae, T. Sanniccolo and J. C. Grossman, *ACS Appl. Mater. Interfaces*, 2020, **12**, 17909–17920.
- (13) D. Y. Choi, H. W. Kang, H. J. Sung and S. S. Kim, *Nanoscale*, 2013, **5**, 977–983.
- (14) I. S. Jin, H. D. Lee, S. Il Hong, W. Lee and J. W. Jung, *Polymers*, 2021, **13**, 586.
- (15) J. Idier, W. Neri, C. Labrugere, I. Ly, P. Poulin and R. Backov, *Nanotechnology*, 2016, **27**, 105705–105712.
- (16) Y. M. Kim, B. Y. Hwang, K. W. Lee and J. Y. Kim, *Nanomaterials*, 2018, **8**, 321.
- (17) F. Duan, W. Li, G. Wang, C. Weng, H. Jin, H. Zhang and Z. Zhang, *Nano Res.*, 2019, **12**, 1571–1577.
- (18) A. Madeira, M. Plissonneau, L. Servant, I. A. Goldthorpe and M. Tréguer-Delapierre, *Nanomaterials*, 2019, **9**, 13–16.
- (19) C. Cai, F. Jia, A. Li, F. Huang, Z. Xu, L. Qiu, Y. Chen, G. Fei and M. Wang, *Carbon*, 2016, **98**, 457–462.
- (20) B. G. Lewis and D. C. Paine, *MRS Bull.*, 2000, **25**, 22–27.
- (21) D. Alemu, H. Y. Wei, K. C. Ho and C. W. Chu, *Energy Environ. Sci.*, 2012, **5**, 9662–9671.